SAMPLING REQUIREMENTS AND ALIAS-FREE PROCESSING IN STRIPMAP SAS SYSTEMS

MARCIN SZCZEGIELNIAK, DAMIAN SZCZEGIELNIAK

University of Technology and Life Sciences
Kaliskiego 7, 85-792 Bydgoszcz, Poland
szczegielniakm@utp.edu.pl, dszczeg@utp.edu.pl

Synthetic Aperture Sonar (SAS) is the high-resolution acoustic imaging technique which allows us to improve along-track resolution. In the era of digital processing, the proper sampling of signals and alias-free processing have an enormous influence on the efficiency of modern SAS systems. SAS processing without taking into account the aliasing phenomenon can cause a serious degradation of the reconstructed SAS image. Therefore, understanding the causes of this phenomenon in real SAS systems and ways of suppressing or avoiding its harmful effects seems to be indispensable. The aim of this paper is the comprehensive discussion of the along-track sampling problem, taking into account the slow-time Doppler support of the raw SAS signal, along-track mapping, effective target area and spatial filtering process as well as practical limitations of the along-track sampling connected with the SAS platform velocity or an maximum unambiguous range to imaged objects. The discussion was extended by mathematical dependencies derived or presented by authors. Moreover, numerical simulations in the Matlab environment was carried out by authors and the results are presented and discussed in this paper. The received raw signal was generated for a stripmap SAS system. Then, the spatial filtering by means of the Polar Formatting with the subdivision of the synthetic aperture was applied to filter out undesirable SAS signal contributions - the reason of the aliasing appearance in real SAS images. The final reconstructed SAS images were obtained by the ω-k algorithm. The carried out experiments confirmed the effectiveness of the presented approach for assumed SAS system parameters.

INTRODUCTION

In order to specify some of the along-track sampling requirements of an SAS system it is indispensable to derive the slow-time Doppler support of the received raw SAS signal, which will be done in the first sections. However, applying the Nyquist sampling rate does not guarantee further alias-free processing. The size of the effective target area in an along-track direction in comparison with the length of the synthetic aperture has to be taken into account as well.

The aliasing problem is also connected with the specific method of data gathering for finite target areas in the stripmap mode and the necessity to filter out unwanted contributions from targets lying beyond the imaged area. It is easy to note in Fig. 1 that in the stripmap mode the received raw SAS signal always includes echoes from outside of the assumed imaged area (marked in gray) because of the antenna beamwidth in the along-track direction (including side lobes of a sonar radiating pattern). It is crucial for alias-free processing in this mode to filter out harmful contributions from the outside. The spatial filtration (often called digital spotlighting) along with dividing the synthetic aperture into smaller subapertures can be applied effectively in the stripmap mode, which was confirmed by the results of the numerical simulations presented in this paper.

One along-track sampling constraint in the context of the velocity of the platform (carrying the sonar) is another practical problem for more distant imaged target areas. Applying a multiple-receiver antenna array seems to be a natural choice to overcome this constraint.

All these issues connected with sampling requirements as well as avoiding aliasing in SAS processing will be discussed in detail in particular sections of this paper.

1. SLOW-TIME DOPPLER SUPPORT OF SAS SIGNAL

In general, a received and demodulated echo signal from an imaged area in the stripmap SAS system can be written as

$$e(\omega, y') = P(\omega)\sum_i \rho_i \cdot a(\omega, x_i, y_i - y') \cdot \exp\left[- j2k \cdot \sqrt{x_i^{\,2} + (y_i - y')^2} \right] \tag{1}$$

where (x_i, y_i) are coordinates of the i^{th} scatterer, $a(\omega, x_i, y_i - y')$ is the transmit-receive mode amplitude beam pattern of the applied antenna, the ρ_i represents an unknown reflectivity of the i^{th} object which can be estimated by a reconstruction algorithm. $P(\omega)$ is the Fourier transform of the transmitted Linear Frequency Modulated (LFM) signal.

The synthetic aperture domain (the y coordinate of the antenna) will be represented by the variable y' in order to distinguish it from the y_i coordinate of targets. It is worth mentioning that the x domain denotes the slant range because it is the two-dimensional representation of the three-dimensional case (which allows us to simplify further analysis, but results can be generalized to the spacial case). Taking advantage of the method of the stationary phase we can evaluate the Fourier transform of the equation 1 with respect to along-track y'. Then we have

$$e(\omega, k_{y'}) = P(\omega)\sum_i \rho_i \cdot A(\omega, k_{y'}) \cdot \exp\left[- j\sqrt{4k^2 - k_{y'}^{\,2}} \cdot x_i - jk_{y'} \cdot y_i \right] \tag{2}$$

where $A(\omega, k_{y'})$ is the slowly-varying transmit-receive mode amplitude pattern in the slow-time Doppler domain and is a simply scaled version of the $a(\omega, x_i, y_i - y')$ component (A(·) and a(·) are not Fourier transform pairs).

$$a(\omega, x, y) \approx \frac{1}{x^2 + y^2} A(\omega, \frac{2ky}{\sqrt{x^2 + y^2}}) \tag{3}$$

The factor $1/(x^2+y^2)$ is not crucial in the further analysis and can be neglected for notational simplicity. The slow-time support band of the of the signal described by the equation 2 is

$$k_{y'} \in \left[-2k \sin\theta_{\max}, 2k \sin\theta_{\max}\right] \tag{4}$$

where θ_{max} is the largest aspect angle of targets with respect to the sonar position y'.

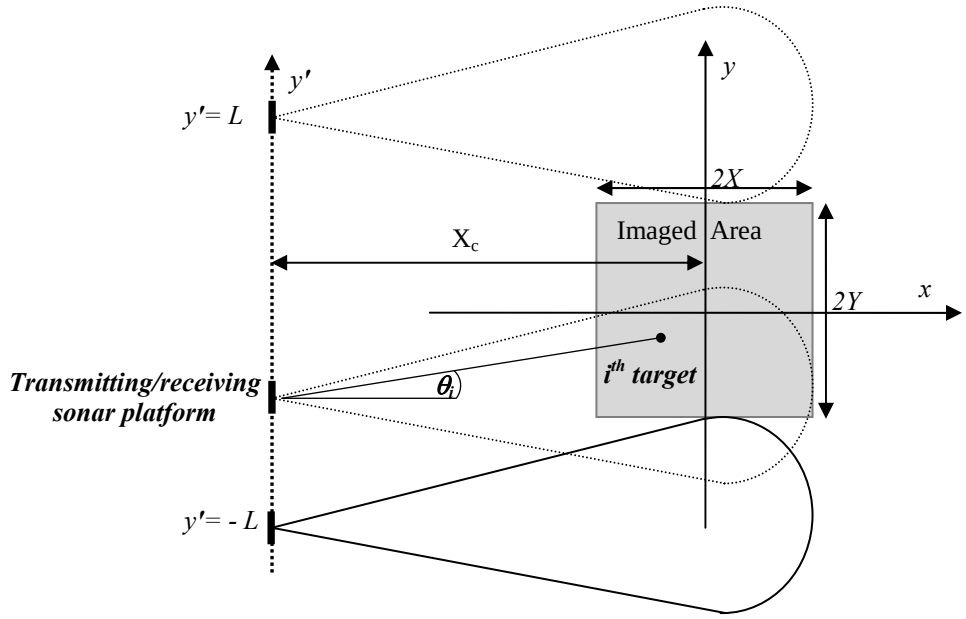

Fig. 1. Imaging scenario for a synthetic aperture system in the stripmap mode.

In the case of the stripmap mode the maximum value of this angle is defined by the angular resolution of the applied antenna. For the real rectangle aperture of the length $D_{y'}$ (in the along-track direction) the angle $\theta_{\max} = \theta_{an}$ can be approximated as [7]

$$\theta_{an} = \arcsin\left(\frac{\lambda}{D_{y'}}\right) \approx \frac{\lambda}{D_{y'}}[rad] \tag{5}$$

where λ is the wavelength. For example, θ_{an} =5,37° for λ=1.5cm and $D_{y'}$=16cm. Then, every target in the imaged area is illuminated within the aspect angles' range

$$\theta \in \left[-\theta_{an}, \theta_{an}\right] \tag{6}$$

It is worth mentioning that the fast-time support band of the stripmap SAS signal is $\omega \in \left[\omega_c - \omega_b, \omega_c + \omega_b\right]$ where ω_c is the applied carrier frequency and $\pm\omega_b$ is the fast-time half bandwidth of the signal.

2. SLOW-TIME SAMPLING REQUIREMENTS

Generally, taking into account the slow-time support band of the stripmap SAS signal represented by equation 4 we can define the Nyquist sampling constraint in the synthetic aperture domain for a given fast-time frequency ω (or wave number *k*) as

$$\Delta y' \le \frac{2\pi}{4k\sin\theta_{an}} \tag{7}$$

By means of equation 5 we can simplify it to the following form

$$\Delta y' \le \frac{\lambda}{4\sin\theta_{an}} = \frac{2\pi}{4\cdot(\lambda / D_{y'})} = \frac{D_{y'}}{4} \tag{8}$$

It is important to note that the sampling criterion in the stripmap mode (in the case of the rectangular real aperture of the antenna) does not depend on the sonar fast-time frequency ω. It is not true for the spotlight mode where "the worst case" is always assumed to define the smallest $\Delta y'$ – the maximum frequency $\omega_{\max}$ ($k_{\max}$ or the minimum value of $\lambda_{\min}$).

3. ALONG-TRACK MAPPING AND ALIASING

Despite applying the proper sampling criterion defined in the last section, undesired aliasing may appear in further digital processing. Because the length of the synthetic aperture is *2L,* the sample spacing in the $k_{y'}$ domain is

$$\Delta k_{y'} = \frac{\pi}{L} \tag{9}$$

On the other hand, the size of the imaged area in the *y* direction is *2Y* and therefore, in order to avoid aliasing the following condition (the Nyquist rate, in fact) has to be satisfied

$$\Delta k_{y} \le \frac{\pi}{Y} \tag{10}$$

The along-track mapping (for example, Stolt mapping, used in the wavenumber reconstruction algorithm) $k_y = k_{y'}$ means that aliasing may appear when the imaged area in cross-range direction *2Y* is larger than the length of the synthetic aperture *2L*. Then the sample spacing $\Delta k_{y'}$ is not sufficient. To avoid aliasing in the k_y domain in further digital processing (before slow-time DFT of the stripmap SAS signal as well as slow-time matched filtering) $e(\omega, y')$ has to be zero, padded in the y' domain, in order to achieve the required sample spacing Δk_y and create the effective aperture L_{eff} equal to length *2Y*. In fact, it is necessary to check and choose the maximum value from these *L* and *Y* figures as the effective synthetic aperture in further SAS processing.

4. EFFECTIVE TARGET AREA

According to equation 6, every target is observable in the same angular period $[-\theta_{an}, \theta_{an}]$, although the antenna beamwidth *2W* in the along-track direction changes with ranges to particular targets as well as with the fast-time frequency of the applied signal. For the rectangular antenna we can write

$$W = \sqrt{x^2 + y^2}\sin\theta_{an} = x\tan\theta_{an} \tag{11}$$

where *W* is half of the beamwidth. Then it is easy to note that every target is observable within the synthetic aperture interval

$$y' = [y_i - W, y_i + W] \tag{12}$$

For the assumed size of the imaged area $2Y$ and for marginal targets (where $y_i = \pm Y$ in along-track direction) we have

$$y' = [-Y - W, Y + W] = [-L, L] \tag{13}$$

But, in fact, the sonar receives echoes from the outside of the imaged region as well

$$Y < |y| \le Y + 2W \tag{14}$$

Therefore, for alias-free SAS processing in the stripmap mode, it is essential to filter out undesirable echoes from the outside of the imaged area which causes the degradation and smearing of the resultant point spread function or background clutter in the reconstructed SAS image. One of the possible solutions here is taking advantage of polar format processing. Actually, it is one of the earlier reconstruction methods which is not particularly precise as a reconstruction algorithm (there are other modern reconstruction algorithms which avoid approximations used in polar format processing) but the low computational cost or the simplicity becomes its benefit in the case of filtration purposes, undoubtedly. We can use an image obtained by means of this algorithm only to filter the SAS signal spatially and then applying another modern reconstruction algorithm (for example, omega-k, range stacking, back projection) to achieve the proper resultant reconstructed SAS image.

The accuracy of the polar formatting depends on a few things which are discussed further.

5. POLAR FORMAT PROCESING FUNDAMENTALS

Transforming the SAS signal given by equation 1 in order to move the origin to the center of the target area (Y_c, X_c), we obtain

$$e(\omega, y') = P(\omega) \sum_i \sigma_i \cdot \exp\left(-j2k\sqrt{(X_c + x_i)^2 + (Y_c + y_i - y')^2}\right) \tag{15}$$

Because we are interested in the fast-varying phase, the slowly-fluctuating $a(\cdot)$ term is neglected here for the notational simplicity of the analysis. It is necessary to note that although we are interested in the broadside imaged area according to Figure 1 (the origin of the coordinate system (x,y) is at $y'=0$) we consider here the squint case which requires the additional term Y_c (see Figure 2). The aim of this manipulation will become further obvious in the subaperture processing (Y_c will be replaced with Y_n , see the section 7).

Let us define the auxiliary function in the form

$$e_a(\omega, y') = P(\omega) \exp\left(-j2k\sqrt{(X_c)^2 + (Y_c - y')^2}\right) \tag{16}$$

which represents the echo from the center of the target area, point $(x_i, y_i)=(0, 0)$. Mixing the complex conjugate of this signal with the equation 15 we get

$$\begin{aligned} e_c(\omega, y') = e(\omega, y') \cdot e_a(\omega, y')^* = |P(\omega)|^2 \sum_i \sigma_i \cdot \exp\left(-j2k\sqrt{(X_c + x_i)^2 + (Y_c + y_i - y')^2}\right) \\ \cdot \exp\left(j2k\sqrt{(X_c)^2 + (Y_c - y')^2}\right) \end{aligned} \tag{17}$$

It is possible to approximate the phase function by

$$\begin{aligned} \exp\left(-j2k\sqrt{(X_c + x_i)^2 + (Y_c + y_i - y')^2}\right) \approx \exp\left(-j2k\sqrt{(X_c)^2 + (Y_c - y')^2}\right) \\ \cdot \exp\left(-j2k(x_i \cos\phi + y_i \sin\phi)\right) \end{aligned} \tag{18}$$

where the angle $\phi = f(y') = \arctan\left(\dfrac{Y_c - y'}{X_c}\right)$.

The meaning of this approximation is explained in Figure 2 and the equation below.

$$\sqrt{(X_c + x_i)^2 + (Y_c + y_i - y')^2} \approx A + B = \sqrt{(X_c)^2 + (Y_c - y')^2} + x_i \cdot \cos\phi + y_i \cdot \sin\phi \quad (19)$$

As we can see the approximation is equivalent to neglecting the wavefront curvature. Then, using this approximation we have

$$\begin{aligned} e_c(\omega, y') &= |P(\omega)|^2 \sum_i \sigma i \cdot \exp(-j2k \cdot x_i \cos\phi - j2k \cdot y_i \sin\phi) = \\ &= |P(\omega)|^2 \sum_i \sigma_i \cdot \exp(-jk_x \cdot x_i - jk_y \cdot y_i) \end{aligned} \quad (20)$$

where the right side of equation 20 can be interpreted as the desired target function in the spatial frequency domain where

$$\begin{aligned} k_x(\omega, y') &= 2k\cos\phi \\ k_y(\omega, y') &= 2k\sin\phi \end{aligned} \quad (21)$$

The two-dimensional Fourier transform will give us the information about the location of targets (x_i,y_i) (which is encoded in the phase function of equation 20) as well as the unknown reflectivity σ_i. We can note as well that the two-dimensional Fourier transform of equation 20 yields the signal in (t, $k_{y'}$) domain (where the transform from ω into t is the inverse one). It will be used in the spatial filtering and discussed in the next section.

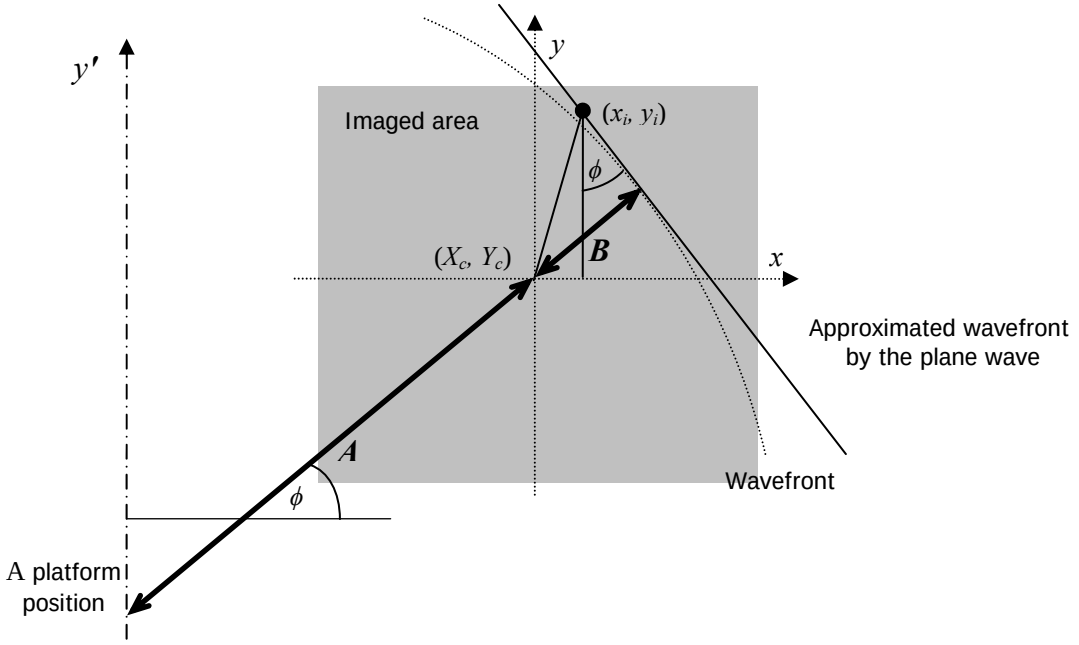

Fig. 2. The plane wave approximation.

However, digital DFT processing requires uniformly distributed data on a rectilinear grid. The name of the polar format processing comes from the fact that the signal in the (ω, y') domain is mapped into polar samples in the spatial frequency domain (k_x, k_y) . To be fully precise, the angle ϕ is not a linear function of the variable y' and therefore, it is not exactly polar format mapping. In any case, it is necessary to interpolate the data on the rectilinear grid before any DFT processing. But we could apply additional approximations called narrow-bandwidth and narrow-beamwidth approximations for the near-broadside case in order to reduce this mapping into the following form (an accurate analysis of these approximations can be found in [2])

$$k_x(\omega, y') \approx 2k \cdot \cos\alpha_c$$
$$k_y(\omega, y') \approx 2k_c \sin\alpha_c - 2k_c \frac{\cos^2\alpha_c}{R_c} \quad \text{where } \alpha_c = \operatorname{artan}\left(\frac{\mathrm{Y_c}}{\mathrm{X_c}}\right) \text{ and } R_c = \sqrt{\mathrm{X_c} + \mathrm{Y_c}} \tag{22}$$

It is necessary to note that the angles α_c and R_c are constants and do not depend on the synthetic aperture y'. The biggest advantage of this mapping is that we do not need interpolation anymore in order to place the data on the evenly spaced grid. This operation is reduced here to the casual scale change.

6. FILTERING OUT UNWANTED CONTRIBUTIONS

As it was mentioned in section 4, the spatial filtering step in the stripmap SAS system is indispensable because of the specific way of data collection. However, due to the polar format processing applied as the reconstruction method, we can take advantage of this algorithm only to filter out the unwanted contributions from targets beyond the illuminated area [2]. Assuming the following limited target area

$$x \in [X_c - X, X_c + X] \wedge y \in [Y_c - Y, Y_c + Y] \tag{23}$$

the SAS raw signal contains the contributions from targets which are located at

$$x \in [X_c - X, X_c + X] \wedge y \in [Y_c - Y - 2W, Y_c + Y + 2W] \tag{24}$$

where W is the sonar half-beamwidth in the along-track direction (along y axis) and depends on the system parameters and range to targets. For the targets defined by the polar spatial coordinates $[\phi_i, r_i]$ when the sonar is at y'=0, the contributions appear at [2]

$$t_i \approx \frac{2r_i}{c} \quad \wedge \quad k_{y'i} \approx 2k_c \sin(\phi_i - \alpha_c) \tag{25}$$

in the polar format processed SAS image (in the time domain t and the spatial frequency $k_{y'}$). Using rectilinear coordinates we get

$$x_i = \frac{c \cdot t_i}{2}\cos(\phi_i + \alpha_c), \; y_i = \frac{c \cdot t_i}{2}\sin(\phi_i + \alpha_c), \quad \text{where} \quad \phi_i = \arcsin\left(\frac{k_{y'i}}{2k_c}\right) \tag{26}$$

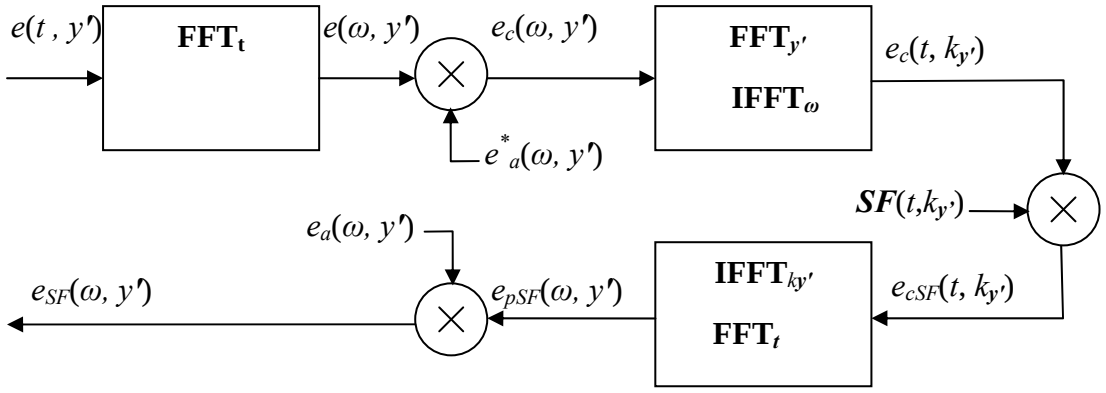

Fig. 3. Spatial filtering scenario.

Finally, the spatial filter (SF) for the polar format processed SAS image, in the (t, $k_{y'}$) domain, takes the form

$$SF(t,k_{y'}) = \begin{cases} 1 \ for \ \left|\frac{c\cdot t}{2}\cos(\phi+\alpha_c) - X_c\right| < X \ \wedge \ \left|\frac{c\cdot t}{2}\sin(\phi+\alpha_c) - Y_c\right| < Y \\ 0 \ otherwise \end{cases} \quad (27)$$

The spatial filtering algorithm was summarized in Figure 3.

7. SUBAPERTURE PROCESSING

Actually, the presented diagram 3 should be supplemented with the option of upsampling (or downsampling after decompression) in the y' domain because of a wider slow-time Doppler bandwidth of $e_c(\omega, y')$ in comparison with $e(\omega, y')$. In fact, mixing the signal $e(\omega, y')$ with the complex conjugate of auxiliary signal 16, often called slow-time compression, may be used in a spotlight system to reduce the sampling rate of the synthetic aperture. This is not true in the stripmap mode because this operation increases the slow-time Doppler bandwidth of the processed signal $e_c(\omega, y')$. To compare with equaton 8, the required Nyquist sample spacing for the compressed signal is [2]

$$\Delta y_c' \le \frac{\lambda}{8\sin\theta_{an} + 4\sin\theta_{\max}} \quad (28)$$

where θ_{max}=arctan(Y/x_{min}) is the maximum aspect angle of the target area when the sonar is at y'=0. It is easy to note that this is more a restrictive sampling criterion. However, the stripmap collected SAS data is not aliased (and assuming the right sampling rate discussed above) it should be upsampled before slow-time compression, which results from the wider bandwidth and equation 28.

It is possible to mitigate this requirement by dividing the synthetic aperture into smaller apertures L_{sub} and then applying the spatial filtering for particular subapertures separately. If the size of subapertures L_{sub} <<L then $\Delta y_c' \approx \Delta y$, there is no need to upsample the signal.

Moreover, another important benefit is that spatial filtering becomes more precise at smaller L_{sub} because of the range migration reduction in small subapertures. To be more precise, the fast-time t_i of the echo arrival from the i^{th} target, approximated by equation 25, becomes more accurate. On the other hand, when the length of the synthetic aperture y'= [$-L$, L] is significant t_i cannot be used as a fast-time measure and a good approximation for the i^{th} target anymore than for all y'.

In Figure 4 we can compare the spatial filtering process with 2 and 4 subapertures. In the case of only 2 subapertures (Fig. 4D) we can note that one desirable target (lying in the imaged scene) was not focused properly, as well as the contribution from the unwanted target is still present (it was not filtered out entirely). Applying 4 subapertures increases the precision of spatial filtering, there are no unwanted contributions, only desirable and well-focused point targets (Fig. 4E).

In practice, the choice of the subaperture size is a kind of tradeoff and it is limited from below, of course. The usage of overly small subapertures is equivalent to the application of overly short rectangular windows whose main lobes $\pm\pi/L_{sub}$ in $k_{y'}$ domain, become more dominant than the bandwidth of the slow-time compressed signal $e_c(\cdot)$. For a particular subaperture [Y_n-L_{sub}, Y_n+L_{sub}], n=1...N_{sub} the spatial filter takes the form of

$$SF_n(t,k_{y'}) = \begin{cases} 1 \ for \ \left|\frac{c\cdot t}{2}\cos(\phi+\alpha_{cn}) - X_c\right| < X \ \wedge \ \left|\frac{c\cdot t}{2}\sin(\phi+\alpha_{cn}) - Y_n\right| < Y \\ 0 \ otherwise \end{cases} \quad (29)$$

where $\alpha_{cn} = \text{artan}\left(\frac{\text{Y}_\text{n}}{\text{X}_\text{c}}\right)$ and $\phi = \arcsin\left(\frac{k_{y'}}{2k_c}\right)$.

8. ALONG-TRACK SAMPLING VS VELOCITY OF PLATFORM

The Pulse Repetition Frequency (PRF) represents the number of along-track samples per unit of slow time and can be defined for a moving sonar platform as

$$PRF = \frac{\text{V}_\text{p}}{\Delta y'} \tag{30}$$

where V_p is the velocity of the platform in the along-track direction. Alternatively, we can use PRI (Pulse Repetition Interval) which is the time interval between successive pulses. PRF is limited by the maximum unambiguous range which can be defined as

$$R_{\max} = \frac{c}{2} \cdot \frac{1}{PRF} = \frac{c}{2} \cdot PRI \tag{31}$$

where c is the sound speed in the water. Comparing these simple equations 30 and 31 we can determine the velocity of the platform V_p

$$\frac{c}{2R_{\max}} = \frac{\text{V}_\text{p}}{\Delta y'} \Rightarrow \text{V}_\text{p} = \frac{c \cdot \Delta y'}{2R_{\max}} \tag{32}$$

We can note that the velocity is the decreasing function of the range R_{max}. A too low velocity can reduce the stability of the platform and make it difficult to maintain a straight course [1]. For example, for the KiwiSAS-III system with sample spacing $D_{y'}/4$, travelling at a velocity of 2m/s, the maximum unambiguous range is only 30m. For more distant target areas we have to reduce the velocity of the platform carrying the sonar, which can be a problem in practice. One could take advantage of orthogonal signals similar to some space-borne SAR systems. However, this solution causes a degradation in SNR [5]. An alternative is to use a multiple-receiver array [6] [1] (many receivers spaced out in the along-track direction) which allows us to increase the along-track sampling rate for more distant target areas at the same and realistic velocity of the platform. An example of this kind of multiple-receiver array for five elements was depicted in Figure 5. The transmitter (the central hydrophone number 3) sends the sound pulses and returned echoes and are received by all hydrophones (number 1-5). The idea of this attitude is to combine echoes from all receivers in order to form the single-receiver data equivalent. Then, we can use standard SAS reconstruction algorithms (for one collocated virtual transmitter/receiver) in further processing. We can easily combine echoes from all receivers into the one-receiver-like signal in $(\omega, k_{y'})$ domain in the following way

$$e(\omega, k_{y'}) = \sum_{h=1}^{H} e_h(\omega, k_{y'}) \cdot \exp(-j\frac{d_h}{2} \cdot k_{y'}) \quad for\ -\frac{k_{y's}}{2} \le k_{y'} < \frac{k_{y's}}{2} \tag{33}$$

where $k_{y's} = 2\pi H / \Delta y'$, h is the index and H is number of the hydrophones, d_h is the distance between the h^{th} hydrophone and the transmitter (for example, d_1 is depicted in Figure 5). The presented approach is based on the phase centers concept well-known from Vernier arrays. For example, the phase centre for the first hydrophone appears in the halfway (the distance $d_1/2$) from the transmitter 3. Other phase centers (for other hydrophones) were determined in the same way and are depicted in Figure 5. We can treat these phase centers as pseudo collocated transmitter/receiver pairs for which the path length can be approximated as the double distance from a particular pair to a target.

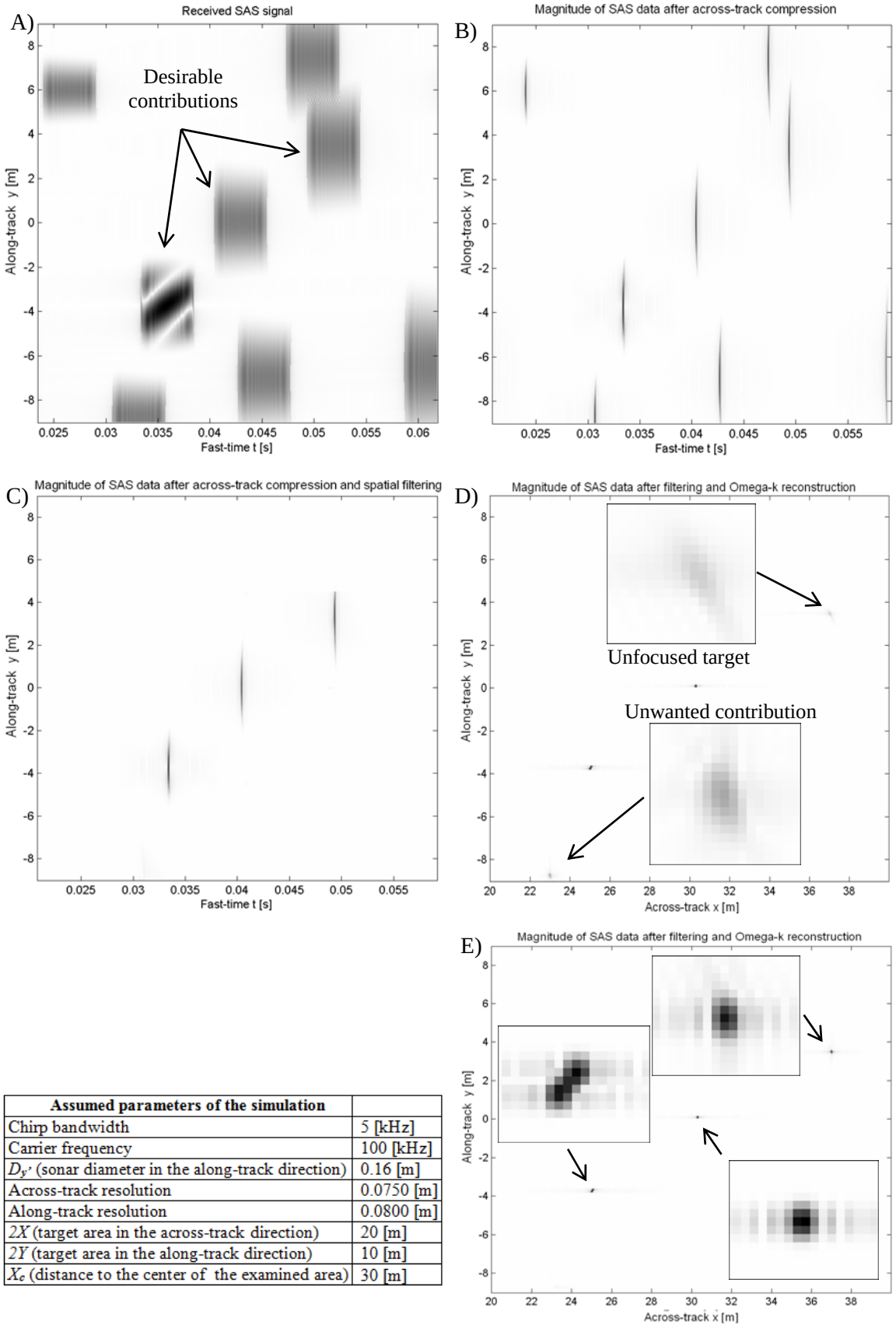

Assumed parameters of the simulation	
Chirp bandwidth	5 [kHz]
Carrier frequency	100 [kHz]
$D_{y'}$ (sonar diameter in the along-track direction)	0.16 [m]
Across-track resolution	0.0750 [m]
Along-track resolution	0.0800 [m]
$2X$ (target area in the across-track direction)	20 [m]
$2Y$ (target area in the along-track direction)	10 [m]
X_c (distance to the center of the examined area)	30 [m]

Fig. 4. Spatial filtering by means of Polar Format Processing A) Received raw SAS signal B) SAS signal after pulse compression C) SAS signal after pulse compression and spatial filtering D,E) SAS signal after full processing (2 and 4 subapertures for D and E respectively).

Actually, this approximated double distance for every pair is vitiated by path length error (the real path length from the transmitter to a target and then back to the receiver is usually different than the approximated double distance from the phase centre to the target) what has to be compensated for every pair separately before combining echoes from all receivers. Using the narrow-beamwidth approximation we can compensate the path length by following phase corrections

$$e_h(\omega, y') = \tilde{e}_h(\omega, y') \cdot \exp\left[-j2kX_{herr}(y')\right] \tag{34}$$

where X_{herr} is the path length correction function for the h^{th} hydrophone. The narrow-beamwidth compensation assumes that a range to a target x_i is much larger than its cross-range y_i and the synthetic aperture y'. Then, path length differences can be treated as an equivalent timing-error in the raw SAS data

$$e(t, y') = \tilde{e}\left(t - \frac{2X_{herr}(y')}{c}, y'\right) \tag{35}$$

For an SAS system with a wider beamwidth this correction becomes less precise. Then, if the timing-error approximation is not acceptable, a more complicated spatially varying filter should be involved [4].

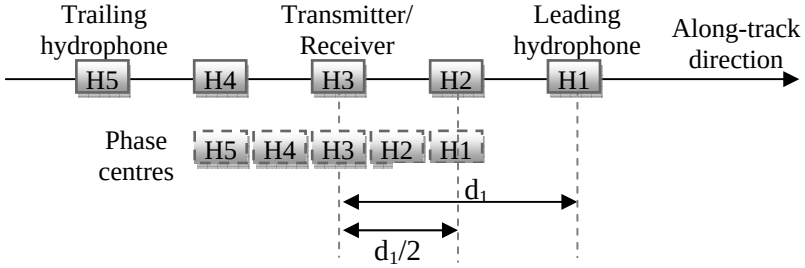

Fig. 5. Multiple-receiver array and its phase centers (the five-receiver case).

It is worth noting that discussed path length corrections can be done by the way of the motion error compensation in the SAS system.

9. CONCLUSIONS AND REMARKS

This paper was an attempt to discuss sampling requirements in along-track direction and alias-free digital processing in synthetic aperture sonar systems in the stripmap mode. The across-track sampling issue was not debated here. However, SAS systems inherit across-track sampling from standard range imaging systems which seems to be well-grounded.

On the basis of the presented slow-time Doppler domain the Nyquist sampling rate in an along-track direction was indicated (sections 1 and 2). Then, attention was paid to Stolt mapping used in the Omega-k reconstruction algorithm (where slow-time Doppler domain $k_{y'}$ is mapped into spatial frequency k_y) and the comparison of two different Nyquist sample spacing requirements, resulting from the length of the synthetic aperture $y'=[-L, L]$ and the size of the target area in the along-track direction $y=[-Y, Y]$. Although the presented dependencies in section 3 are fully valid for every stripmap SAS system, the necessity of zero padding to avoid an aliasing effect rather concerns spotlight modes where the lengths of synthetic apertures L can be much shorter than the size of the imaged scene Y.

However, it is important to be aware of this relationship between L and Y sizes and the aliasing appearance in a stripmap system where the effective target area in the along-track

direction (section 4) y=[$-Y-2W$, $Y+2W$] is wider than [$-L$, L] (compare with equation 13). Moreover, it is worth noting that the occurrence of side lobes in real antennas makes the effective target area even wider.

Although a finite target area is assumed in stripmap SAS systems, echoes are received from outside the imaged region as well. Therefore, spatial filtering before the SAS reconstruction of the imaged scene is crucial to avoid unwanted contributions (coming from objects beyond the target area) and the harmful aliasing effect. Polar format processing fundamentals were presented, as well as the way of enhancing its precision by dividing the synthetic aperture (the subaperture processing).

Numerical spatial filtering by means of polar format processing and dividing the synthetic aperture into smaller subapertures (to enhance the precision of this algorithm) was carried out in the Matlab environment (license number: 260992). All undesirable contributions from targets beyond the assumed along-track interval y=[-5m, 5m] was filtered out in the reconstructed SAS image. We can note in Fig. 4D that dividing the synthetic aperture into only two subapertures did not allow us to achieve satisfying results. Unwanted targets are still present (not filtered out properly) and the desirable targets from the assumed target area were not well-focused (actually, they were affected by an inaccuracy in the filtering process). However, in the case of 4 subapertures we can note a significant improvement in filtering precision, we cannot see any unwanted targets, and desirable point targets are well-focused (Fig. 4E).

In the last section, the along-track sampling constraint for more distant target areas in the context of practical velocities of the SAS platform was discussed. Then, the multiple-receiver array as a solution of this problem was suggested. As was mentioned, the additional processing allows us to create an equivalent one-receiver signal and not to affect further reconstruction algorithms. However, necessary path length corrections have to be carried out for every single receiver beforehand. An SAS system with H receivers can travel H times faster than a single-receiver SAS system with the same along-track resolution [5].

REFERENCES

[1] D.R. Wilkinson, Efficient Image Reconstruction Techniques for a Multiple-Receiver Synthetic Aperture Sonar, MSc thesis, 13-18, Electrical and Electronic Engineering at the University of Canterbury, New Zealand 2001.

[2] M. Soumekh, Synthetic Aperture Radar Signal Processing, John Wiley & Sons, 238-241, 402-411, USA 1999.

[3] M. Szczegielniak, Spatial SAS Signal Filtering by Means of Polar Format Processing, Hydroacoustics, Vol. 9, 191-198, 2005.

[4] M. Szczegielniak, Motion Compensation Problem in Stripmap SAS Systems, Hydroacoustics, Vol. 10, 45-54, 2007.

[5] Hayden J. Callow, Signal Processing for Synthetic Aperture Sonar Image Enhancement, PhD thesis, 23, 24, 29, Electrical and Electronic Engineering at the University of Canterbury, New Zealand 2003.

[6] Roy Edgar Hansen, Hayden John Callow, Challenges in Seafloor Imaging and Mapping With Synthetic Aperture Sonar, 3679, IEEE Transactions on Geoscience and Remote Sensing, Vol. 49, No. 10, October 2011.

[7] Stefan Leier, Abdelhak M Zoubir, Aperture undersampling using compressive sensing for synthetic aperture stripmap imaging, content/2014/1/156, EURASIP Journal on Advances in Signal Processing (2014).